34th EPS Conference on Plasma Phys. Warsaw, 2 - 6 July 2007 ECA Vol.31F, P-4.145 (2007)

Fast Ion Anisotropy Drive for Bi-Directional Tornado Modes on JET

P. Sandquist[1], S.E. Sharapov[2], M. Lisak[1], T. Johnson[3], F. Nabais[4]
and JET-EFDA contributors*

[1]*EURATOM-VR Association, and Department of Radio and Space Science, Chalmers University of Technology, Göteborg, Sweden*

[2]*EURATOM/UKAEA Fusion Association, Culham Science Centre, Abingdon, UK*

[3]*EURATOM-VR Association, Fusion Plasma Physics, KTH, Stockholm, Sweden*

[4]*Euratom/IST Fusion Association, Centro de Fusão Nuclear, Lisboa, Portugal*

**See the Appendix of M. L. Watkins et al., Fusion Energy 2006 (Proc. 21st Int. Conf. Chengdu, 2006) IAEA, (2006)*

1 Introduction

Resonant interaction between shear Alfvén waves and energetic ions is one of the key burning plasma physics issues currently investigated at JET. A loss of the fast ion stabilisation effect on the $n = 1$ kink mode has previously been found [1-4] to correlate with excitation of energetic particle-driven modes inside the $q = 1$ magnetic surface, either $n = 1$ fishbones or higher frequency so-called "tornado" modes. The tornado modes were identified in [5] as Toroidal Alfven Eigenmodes (TAEs) inside the $q = 1$ magnetic surface. The loss of sawtooth stabilisation by fast ions can be understood as the possible effect of multiple-mode structures of tornado modes, observed prior to the sawtooth crashes, on the fast ion confinement [6]. Bi-directional tornado modes with both positive and negative toroidal mode numbers n (i.e. propagating in both co-current and counter-current direction) were observed on JT-60U [1], but remain unexplained so far. In this paper, the first JET observations of bi-directional tornado modes are reported and explained. The spectroscopic analysis of the plasma equilibrium, which is performed with a suite of equilibrium and spectral MHD codes, verifies the observed evolution of tornado mode frequencies and is used to identify the temporal evolution of the safety factor inside $q = 1$ just before the sawtooth crashes. In order to understand the excitation mechanism of bi-directional tornado modes, we follow the idea of [7] and revisit the calculation of linear TAE growth rate due to ICRH-accelerated trapped ions in the small banana width limit [8] and identify a necessary velocity space anisotropy condition for a positive growth rate of bi-directional tornado modes.

2 Experimental Observations on JET

Figure 1 shows the electron temperature, the line-averaged electron density, and power waveforms in JET discharge no. 66203 with a magnetic field of 2.7 T and a 2 MA plasma current. High power ICRH accelerates hydrogen minority ions to the MeV range, whereas NBI-blips are used for ion temperature and safety factor diagnostics. In this discharge, eight monster sawteeth can be observed from the electron temperature measurements of Fig. 1, and all of them are preceded by bi-directional tornado modes as measured by both magnetic pick-up coils and O-mode interferometry — see Fig. 2. The magnetic data in Fig. 2 shows that co-propagating tornado modes in the range $n = 2$ to $n = 9$ as well as counter-propagating tornado modes with $n = -4$ to $n = -6$ are observed. At somewhat lower frequencies, Alfvén cascades can be found in interferometry data, suggesting a possible relation between Alfvén cascades and tornado modes in this case [9].

In Fig. 3, magnetics data for the spectrum of bi-directional tornado modes just before the monster sawtooth crash at $t = 20$ s is presented. Due to the application of NBI

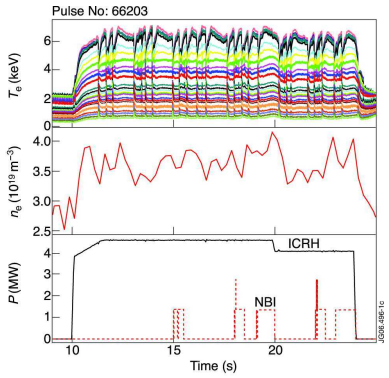

Fig. 1: Top: Electron temperature T_e measured with multi-channel ECE diagnostics at different radii on JET. Middle: Electron density $n_e(0)$ measured with LIDAR. Bottom: ICRH (black) and diagnostic NBI (red) power waveforms.

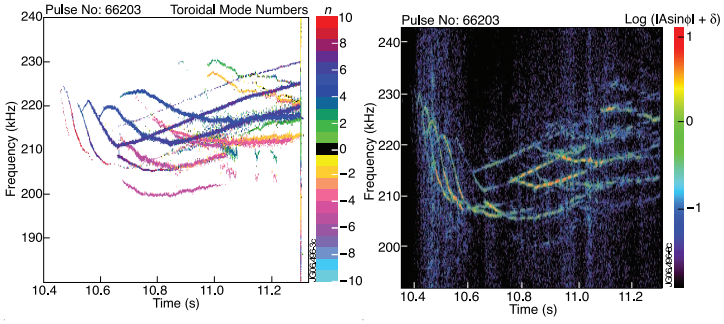

Fig. 2: Left: Magnetic spectrogram showing toroidal mode numbers of the observed bi-directional tornado modes preceding the monster sawtooth crash at 11.3 s. Right: Spectrogram of high-frequency density perturbations measured with the O-mode interferometry, also showing tornado modes in the TAE frequency range around 200–240 kHz.

just before the sawtooth crash (see Fig. 1), NBI-driven toroidal rotation of the plasma causes Doppler shifts in the frequencies of tornado modes with different toroidal mode numbers, leading to a spectral separation between co- and counter-propagating modes.

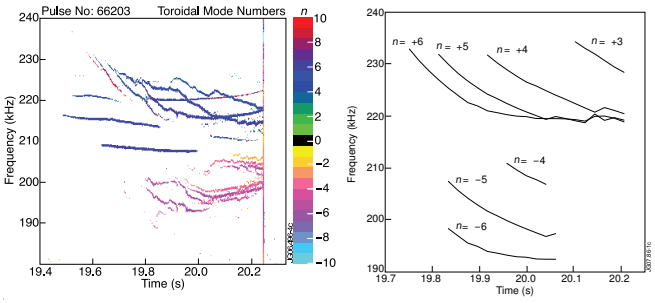

Fig. 3: Left: Magnetic spectrogram showing the temporal evolution of bi-directional tornado modes and TAEs (no chirping) at the time $t = 20.2$ s in JET discharge number 66203. Right: Spectrogram showing the temporal evolution of MHD modelled tornado modes before the sawtooth crash event at $t = 20.2$ s in JET discharge no. 66203. The agreement with experimental data is verified. The observed spectrum is further supported by a velocity anisotropy drive estimate (Sec. 4).

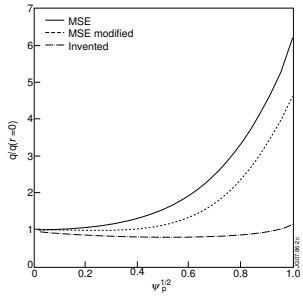

Fig. 4: Normalised safety factor profiles $q(r)$ as functions of normalised poloidal flux, $\psi_p^{1/2} \sim r/a$, where a is the minor radius. The three equilibria are the MSE measured equilibrium (solid line), a non-monotonic modified MSE equilibrium (dashed line) and an equilibrium from JET shot no. 54956 (dash-dotted line).

3 MHD Modelling

The Grad-Shafranov equilibrium solver HELENA [10] and EFIT are first used to reconstruct an equilibrium in straight field line coordinates from one of the three safety factor profiles in Fig. 4. In addition, two reversed shear equilibria are tested. TAEs are then found in the Alfvén continuum gap structure with the MHD spectral code MISHKA [11] for different values of $q(r = 0) = q_0$. When we model the monotonic MSE measured equilibrium, the temporal evolution of the spectrum of bi-directional

tornado modes is found to be in agreement with experimental data, see Fig. 3. Since the modelling of the reversed shear scenarios does not explain the question as how to explain the second group of experimentally observed counter-propagating tornado modes, excited 100 ms before the sawtooth crash in Fig. 3, one concludes that the monotonic q-profile as suggested by MSE is indeed supported by MHD spectroscopy.

4 Fast Ion Anisotropy Drive

It is well known that resonant interaction between TAE instabilities and hot ions can lead to excitation of TAEs if $\omega < \omega_\star$ holds [12], where

$$\beta_{\rm hot} = \frac{8\pi}{B_0^2}\int_{-\pi}^{\pi}\frac{{\rm d}\theta}{2\pi}\int {\rm d}^3 pEf_0\,, \quad \omega_\star = \frac{n}{M\omega_{\rm c}R_0}\frac{\partial f_0/\partial J_\varphi}{\partial f_0/\partial E}. \tag{1}$$

Here, the sign of the hot ion pressure gradient determines whether the excited modes propagate co-current ($n > 0$ for ${\rm d}\beta_{\rm hot}/{\rm d}r < 0$) or counter-current ($n < 0$). In order to support bi-directional tornado modes, the hot ion pressure profile has to be reversed at a radial position inside the $q = 1$ surface, where locally counter-propagating modes can tap energy from the hot ion pressure reversal. However, modelling of the ICRH-accelerated distribution function with the self-consistent code SELFO [13] shows that there is no pressure reversal at the time of tornado mode excitation.

In order to determine the excitation mechanism for bi-directional tornado modes, we revisit the analytic treatment of Ref. [8]. The growth rate of TAEs due to both passing and trapped ions is calculated in three mode width limits. For trapped particles the small banana width approximation is used, the validity of which is confirmed by CASTOR-K [14] modelling for tornado modes with $n > 4$. The obtained analytical expressions for the growth rate of TAEs, which can be found explicitly in [9], only introduce small corrections to previous results [8]. From these expressions, we then investigate the role of hot ion velocity anisotropy [7]. The conditions for excitation of both co- and counter-propagating modes are

$$\partial f_0/\partial\lambda < 0\,, \quad |\partial f_0/\partial\lambda| > \frac{E}{\lambda}\left|\frac{\partial f_0}{\partial E}\left(1-\frac{\omega_\star}{\omega_{\rm r}}\right)\right|\,, \tag{2}$$

where it is assumed that $\partial f_0/\partial E < 0$. We model the ICRH-accelerated protons with a velocity distribution function [7]

$$f_0 = \alpha\beta_{\rm hot}\exp(-E/T)\exp(-(\lambda-\langle\lambda\rangle)^2/2\sigma_\lambda^2) \tag{3}$$

strongly peaked in the pitch angle variable around $\langle\lambda\rangle$. Here, $f_0(\lambda, E)$ is the velocity distribution function of ICRH-accelerated protons, $\lambda = \mu B_0/E$ is the pitch-angle variable, $E = Mv^2/2$ is the ion energy, $\sigma_\lambda \in [0.013, 0.065]$ is the peaking parameter indicating the degree of anisotropy, T is the tail temperature and α is a pressure normalisation constant. The form of the hot ion velocity distribution function in Eq. (3) is suggested by SELFO modelling [13]. Fig. 5 illustrates modelled pitch-angle distribution functions of ICRH-accelerated hot protons for JET shot no. 66203.

From Eqs. (2), we derive a velocity anisotropy criterion for driving tornado modes with negative toroidal mode numbers,

$$\sigma_\lambda^2 < \sigma_{\lambda,{\rm d}}^2 = \left|\frac{T\lambda(\lambda-\langle\lambda\rangle)}{E\left(1-\frac{\omega_\star}{\omega_{\rm r}}\right)}\right|\,. \tag{4}$$

From the output of SELFO, the tail temperature T, the pitch-angle centre $\langle\lambda\rangle$, the 1/e value λ and the energy E of ICRH-accelerated ions can be used, together with the resonant frequency $\omega_\mathrm{r} = \omega_\mathrm{TAE} = v_\mathrm{A}/2qR_0$ and the calculated $\omega_\star$ from Eq. (1), to obtain $\sigma_{\lambda,\mathrm{d}} = [0.0509, 0.0551, 0.0594]$ for $n = [-6, -5, -4]$.

We note that the required change in σ_λ very well explains the experimental observation in Fig. 3 that counter-propagating tornado modes are delayed as compared to co-propagating tornado modes, even though they are associated with the same magnetic flux surface and, hence, the eigenmode solutions appear simultaneously. However, the damping effect due to $\mathrm{d}\beta_\mathrm{hot}/\mathrm{d}r$ is too high for counter-propagating tornadoes to be excited together with their corresponding co-propagating tornadoes. As the value of σ_λ drops below the critical value $\sigma_{\lambda,\mathrm{d}}$, from Eq. (4), the velocity anisotropy drive for counter-propagating tornadoes becomes larger than the universal damping coming from a monotonic hot ion pressure profile. Since the limit for $n = -6$ is the most restrictive, it does not appear ahead of the $n = -5$ and $n = -4$ tornadoes, which would be the case otherwise.

5 Conclusions

Recent observations on JET show that bi-directional tornado modes are excited by trapped ions generated due to ICRH. Modelling with MHD codes determines the radial location, the toroidal mode numbers and the temporal evolution of the modes. Furthermore, the drive mechanism for bi-directional tornado modes is investigated analytically and a condition for positive growth rate of bi-directional tornado modes, in terms of the parameters of the fast ion anisotropic velocity distribution function, is derived and analysed. It is found that the free energy coming from anisotropy of the fast ion velocity distribution function can strongly contribute to the mode excitation. For relevant plasma parameters, it is shown that the excitation condition is satisfied just before a giant sawtooth crash occurs.

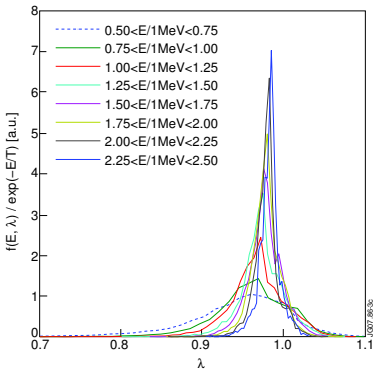

Fig. 5: SELFO modelling output showing the hot ion velocity distribution function at different energies. The form of the hot ion velocity distribution function suggests an analytic model given by Eq. (3).

Acknowledgements

This work has been conducted under association contracts between EURATOM, Portugal, Sweden and UK, and was partly funded by the Swedish Research Council. The work at the UKAEA was partly funded by UK EPSRC.

References

[1] M. Saigusa et al., Plasma Phys. Control. Fusion **40**, 1647 (1998). [2] S. Bernabei et al., Phys. Rev. Lett. **84**, 1212 (2000). [3] W. W. Heidbrink et al., Nuclear Fusion **39**, 1369 (1999). [4] S. E. Sharapov et al., Nuclear Fusion **45**, 1168 (2005). [5] G. J. Kramer et al., Phys. Rev. Lett. **92**, 015001 (2004). [6] S. Bernabei et al., Phys. Rev. Lett. **84**, 1212 (2000). [7] H. V. Wong and H. L. Berk, Phys. Lett. A **251**, 126 (1999). [8] T. Fülöp et al., Plasma Phys. Control. Fusion **38**, 811 (1996). [9] P. Sandquist et al., to be submitted to Physics of Plasmas. [10] G. T. A. Huysmans et al., Proc. CP90 Conf. on Comp. Phys., 371 (1991). [11] A. B. Mikhailovskii et al., Plasma Phys. Reports **23**, 844 (1997). [12] G. Y. Fu and J. W. Van Dam, Phys. Fluids B 1, 1949 (1989). [13] J. Hedin et al., Nuclear Fusion **42**, 527 (2002). [14] D. Borba and W. Kerner, J. Comp. Phys. **153**, 101 (1999).